Contribution from Union Carbide Corporation,
South Charleston, West Virginia 25303

$[Rh_{10}As(CO)_{22}]^{3-}$. Example of Encapsulation of Arsenic by Transition-Metal Carbonyl Clusters As Illustrated by the Structural Study of the Benzyltriethylammonium Salt

JOSÉ L. VIDAL[1]

Received November 19, 1979

The reaction of $Rh(CO)_2acac$ and alkali carboxylates in a glyme solvent with Ph_3As under ~300 atm of carbon monoxide and hydrogen resulted in the isolation of $[PhCH_2N(C_2H_5)_3]_3[Rh_{10}As(CO)_{22}]\cdot C_4H_8O$. The complex has been characterized via a complete three-dimensional X-ray diffraction study. The complex crystallizes in the primitive monoclinic space group $P2_1/n$, with a = 14.785 (2) Å, b = 22.495 (7) Å, c = 23.083 (5) Å, β = 95.45 (1)°, V = 7642.3 Å^3, and δ(calcd) = 2.059 g/cm^3. The structure was solved by direct methods and refined by difference-Fourier and least-squares techniques. All nonhydrogen atoms have been located and refined; final discrepancy indices are R_F = 5.4% and R_{wF} = 6.0% for all 3093 symmetry-independent reflections in the range of $0.5° \leq 2\theta \leq 45°$. The structure consists of a bicapped square antiprism of rhodium atoms with the arsenic atom in its center. Rhodium–rhodium contacts are in the range 2.869–3.120 Å with arsenic–rhodium contacts of 2.502 and 3.008 Å for the metal atoms on the prism and the capped corner, respectively. Average values for the rhodium–carbon and carbon–oxygen distances are in the normal range, 1.83 and 1.16 Å, respectively, for the terminal carbonyls. There are one set of symmetrical and another of asymmetrical bridging carbonyls with Rh–C = 1.99 Å and C–O = 1.21 Å for the former set and Rh–C = 2.222 and 1.95 Å and C–O = 1.20 Å for the latter one, as is usual in this situation. High-pressure infrared studies show the cluster is stable under 537 atm of $CO-H_2$ (1:1 ratio) up to 150 °C, but it reacts under 1000 atm, yielding $[Rh(CO)_4]^-$ and $[Rh_9As(CO)_{21}]^{2-}$. The reaction of these two anions to form the initial anion has also been established.

Introduction

Several examples of transition-metal carbonyl clusters containing encapsulated or interstitial atoms of main-group elements have been recently reported by this laboratory. Specifically it has been shown that rhodium carbonyl clusters are able to accommodate atoms of the elements in groups 5 and 6 in their polyhedral cavities, as illustrated by $[Rh_9P(CO)_{21}]^{2-}$ and $[Rh_{17}S_2(CO)_{32}]^{3-}$, respectively.[2,3] These clusters have exhibited some unusual properties. They are more stable than rhodium carbonyl clusters in which there is not a heteroatom present, e.g., $[Rh_{13}(CO)_{24}H_3]^{2-}$, which transform under carbon monoxide and hydrogen into $[Rh_5(CO)_{15}]^-$ and $[Rh(CO)_4]^-$.[4] Also, the presence of a somewhat peculiar localized carbonyl scrambling was detected for $[Rh_{17}S_2(CO)_{32}]^{3-}$,[5] while the mobility of the metal skeleton present in $[Rh_9P(CO)_{21}]^{2-}$[6] has been previously found only in one instance.[7]

The influence of the nature of the encapsulated main-group atom(s) on the behavior of the clusters is an obvious potential feature of this chemistry.[8] It could be expected that variations in the steric demands, electronegativity, and the number of valence electrons of these atoms would be reflected by either cluster structure or reactivity.

The previous existence of $[Rh_9P(CO)_{21}]^{2-}$ and the similarities in the reactivity of ligands containing group 5 donor atoms[9] prompted us to test the ability of other elements of this group to form similar clusters. Arsenic was chosen because its covalent radius (1.24 Å) is close to but larger than that of phosphorus (1.10 Å).[10] This gradual increase in the size of the encapsulated atom was preferred as a way of testing the effects of its steric demands in the cluster polyhedra, since it was expected that modification of the packing of metal atoms could result in this way.[11] The ability of atomic arsenic to act as a ligand toward transition metal atoms was shown for $Co_2(CO)_6As_2$,[12] $As_3Co(CO)_3$,[13] $[Ni_4(\eta^5\text{-}C_5H_5)_4(\mu_3\text{-}As)_3]^+$,[14] $[Co_4(\eta^5\text{-}C_5H_5)_4(CO)_4(\mu_3\text{-}As)]^+$,[15] $Fe_3(CO)_9(\mu_3\text{-}As)_2$,[16] and $As_2Fe_3(CO)_{11}$.[17] These examples cover several group 8 metals, and they suggested that a related reactivity could be found with other elements of the same group such as rhodium. Similar arguments were used in the case of phosphorus prior to the synthesis of $[Rh_9P(CO)_{21}]^{2-}$[2] and $[Rh_{10}P(CO)_{22}]^{3-}$.[19]

It has been previously proved in this laboratory that successive losses of phenyl radicals from triphenylphosphine result in "naked" phosphorus and in the formation of $[Rh_9P(CO)_{21}]^{2-}$ and $[Rh_{10}P(CO)_{22}]^{3-}$.[2,19] The lower strength of the arsenic–carbon linkage with respect to the phosphorus–carbon[10] linkage indicated that such reactivity should be even easier in the case of arsenic. It was therefore expected that the arsenic analogue of the phosphido clusters above could be prepared under reaction conditions similar to those previously reported for these species, but using triphenylarsine.

The preparation and characterization of $[Rh_{10}As(CO)_{22}]^{3-}$ is described in this work. This cluster contains an arsenic atom placed inside the cluster's cavity. It illustrates the ability of arsenic to parallel the chemistry previously reported for phoshorus. It also provides the first example of the ability of atomic arsenic to share all of its valence electrons, as previously established for phosphorus[3,19] and sulfur.[2]

(1) The structure of the cluster has been solved by Dr. Jan Troup of Molecular Structure Corp.
(2) J. L. Vidal, R. A. Fiato, L. A. Cosby, and R. L. Pruett, *Inorg. Chem.*, **17**, 2574 (1978).
(3) J. L. Vidal, W. E. Walker, R. L. Pruett, and R. C. Schoening, *Inorg. Chem.*, **18**, 254 (1979).
(4) J. L. Vidal and W. E. Walker, *Inorg. Chem.*, **19**, 894 (1980).
(5) J. L. Vidal, R. A. Fiato, R. L. Pruett, and R. C. Schoening, *Inorg. Chem.*, **18**, 1821 (1979).
(6) O. Gansow, R. C. Schoening, and J. L. Vidal, *J. Am. Chem. Soc.*, in press.
(7) C. Brown, B. T. Heaton, P. Chini, A. Fumagalli, and G. Longoni, *J. Chem. Soc., Chem. Commun.*, 309 (1977).
(8) J. L. Vidal, W. E. Walker, R. A. Fiato, R. L. Pruett, and R. C. Schoening, "Proceedings of the First International Symposium on Homogeneous Catalysis", Marcel Dekker, New York, 1979.
(9) R. J. Cross, *Int. Rev. Sci.: Inorg. Chem., Ser. Two*, **5**, 147 (1974).
(10) F. A. Cotton and G. Wilkinson, "Advanced Inorganic Chemistry", 3rd ed., Wiley, New York, 1972.
(11) (a) P. Chini, G. Longoni, and V. G. Albano, *Adv. Organomet. Chem.*, **14**, 285 (1976); (b) S. Martinengo, G. Ciani, A. Sironi, B. T. Heaton, and J. Mason, *J. Am. Chem. Soc.*, **101**, 7095 (1979).
(12) A. S. Foust, M. S. Foster, and L. F. Dahl, *J. Am. Chem. Soc.*, **91**, 5633 (1969).
(13) A. S. Foust, M. S. Foster, and L. F. Dahl, *J. Am. Chem. Soc.*, **91**, 5631 (1969).
(14) J. D. Sinclair and L. F. Dahl, to be submitted for publication.
(15) C. F. Campana and L. F. Dahl, *J. Organomet. Chem.*, **127**, 209 (1977).
(16) L. T. J. Delbaere, L. J. Kruczynski, and D. W. McBride, *J. Chem. Soc., Dalton Trans.*, 307 (1973).
(17) W. Hieber, J. Gruber, and F. Lux, *Z. Anorg. Allg. Chem.*, **300**, 275 (1959).
(18) A. Vizi-Orosz, V. Galamb, G. Palyi, L. Marko, G. Bor, G. Natile, *J. Organomet. Chem.*, **107**, 235 (1976).
(19) J. L. Vidal, W. E. Walker, and R. C. Schoening, *Inorg. Chem.*, companion paper in this issue.

0020-1669/81/1320-0243$01.00/0

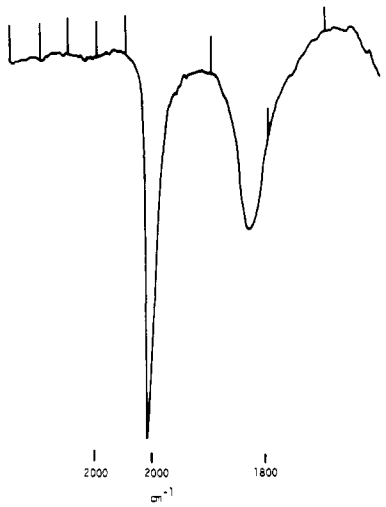

Figure 1. Infrared spectrum of the $[C_6H_5CH_2N(C_2H_5)_3]^+$ salt of $[Rh_9As(CO)_{21}]^{2-}$ in acetone solution.

Experimental Section

The reagents used in this work were obtained from the same sources as before;[2,3] triphenylarsine was supplied by Aldrich Chemical Co., and it was used without purification. The experimental procedures were similar to those already described.[2-4] Crystals were obtained by the slow-diffusion method using acetone–2-propanol. The crystal and molecular structures were determined by Molecular Structure Corp., College Station, Texas.

Syntheses of $[Rh_9As(CO)_{21}]^{2-}$ and $[Rh_{10}As(CO)_{22}]^{3-}$ Salts. $Rh(CO)_2acac$ (12.06 g, 46.59 mmol) and cesium benzoate (2.783 g, 11.02 mmol) were dissolved in 1 L of tetraethylene glycol dimethyl ether. Triphenylarsine (4.28 g, 13.98 mmol) was added to the solution and the mixture was stirred under argon for 0.5 h. The final solution was charged to a previously evacuated high-pressure autoclave, which was then pressurized to approximately 250 atm with carbon monoxide and hydrogen in a 1:1 molar ratio. The temperature was then raised to 140–160 °C, and the reaction was allowed to continue overnight, while being stirred. The resulting solution was collected into a 1.5-L Schlenk receiver, after being cooled under pressure to 50 °C. The mixture was filtered, and the filtrate was treated with toluene in a 10:1 ratio. The solvent was decanted, and the resulting oil was redissolved in acetone or in tetrahydrofuran. The filtered extract was then treated with a 2-propanol solution of benzyltriethylammonium chloride (1 g in 15 mL) in 1:1 volume ratio. The solid formed was separated by filtration, washed with fresh 2-propanol, and vacuum-dried. The product (3.18 g) corresponded to a yield of 28.8% based on rhodium. The tetraalkylammonium and benzyltriethylammonium salts of this anion are soluble in acetone, acetonitrile, and similar solvents but show either slight solubility or insolubility in less polar solvents. The cesium salt, by contrast, is soluble in those solvents and in methanol, tetrahydrofuran, and 1,4-dioxane, as well as in glymes. Anal. Calcd for $Rh_{10}AsO_{23}N_3C_{65}H_{74}$: C, 32.95; H, 3.15; N, 1.77; Rh, 43.43; As, 3.16. Found: C, 32.62; H, 3.25; N, 1.68; Rh, 43.49; As, 3.12.

A fourfold excess of hexane was added to the mother liquor of $[C_6H_5CH_2N(C_2H_5)_3]_3[Rh_{10}As(CO)_{22}]$ after this species had been removed. A precipitate was slowly formed. This solid was isolated and treated as already described for the former cluster. The similarity of the infrared spectrum of the benzyltriethylammonium salt of the resulting material with that of $[Rh_9P(CO)_{21}]^{2-}$ (Figure 1) as well as its elemental analysis (see below) strongly suggested this product (5.60 g) was $[C_6H_5CH_2N(C_2H_5)_3]_2[Rh_9As(CO)_{21}]$ isolated in a 55.4% yield based on rhodium. Anal. Calcd: C, 28.91; H, 1.13; N, 1.44; Rh, 47.47; As, 3.84. Found: C, 28.84; H, 1.00; N, 1.52; Rh, 47.40; As, 3.86. Single-crystal X-ray diffraction studies to be reported elsewhere have confirmed the proposed identity for the material.

Another Improved Synthesis of $[Rh_{10}As(CO)_{22}]^{3-}$. The relative low yields of the previous reaction indicated the need of a better synthesis. Another procedure for the preparation of this anion was found following the method previously applied for the preparation of the phosphorus analogue.[19]

$Rh(CO)_2acac$ (12.0 g, 46.5 mmol), cesium benzoate trihydrate (2.80 g, 9.52 mmol), triphenylarsine (4.20 g, 13.97 mmol), and cesium borohydrate (1.50 g, 10.1 mmol) were mixed in 950 mL of tetraethylene glycol dimethyl ether or tetraglyme. This mixture was charged to a high-pressure autoclave by following the procedures described in previous preparations,[2,19] and the system was allowed to react for 2 h under 6000 psig of $CO-H_2$ at 150 °C. The solution was vented to atmospheric conditions afterward, filtered, and precipitated with an eightfold excess of dry toluene. The resulting oil was washed with 2-propanol, dissolved in acetone, and precipitated with a twofold excess of a solution of benzyltriethylammonium chloride in 2-propanol (1 g in 40 mL). The resulting solid was isolated by filtration, washed with 2-propanol, and vacuum dried. This product (11.77 g) has an elemental analysis and infrared and ^{13}C NMR spectra as expected for $[PhCH_2N(C_2H_5)_3]_3[Rh_{10}As(CO)_{22}]$ (vide supra). The yield of this salt based on rhodium was 97.8%.

X-ray Data Collection. The physical characteristics and manipulations of the crystal used in this study were similar to those already described for other clusters.[2,3]

The instrumentation and experimental settings have also been previously described.[2,3] A different incident-beam collimator diameter, 0.7 mm, and a scan range of 4–40°/min were used in this study. The scan was conducted from $[2\theta(Mo\ K\alpha_1) - 0.4]°$ to $[2\theta(Mo\ K\alpha_2) + 0.4]°$ over a data range of $0° < 2\theta(Mo\ K\alpha) < 42°$. Data reduction followed a previous procedure,[2] but an absorption correction was made this time by using the ψ-scan technique. The maximum variation in transmission in a typical ψ scan was 8.67%. The space group $P2_1/n$ was confirmed by data refinement. Twenty-five reflections were used in the determination of the unit cell dimensions (Figure 2). Numerical information on data collection is given in Table I.

Solution and Refinement of the Structure. The hardware and software employed are the same as in previous reports.[2,3] Similarly the scattering factors, the considerations for anomalous dispersion effects, and the discrepancy indices used here have already been described.[2,3]

The structure was solved by direct methods. A total of 16 phase sets was produced by using 355 reflections with $|E_{min}| = 2.15$ and 2000 phase relationships. An E map prepared from the phase set showing the first best probability statistics (absolute figure of merit 1.0067, residual 22.5; both are defined in MULTAN 74 as it is included in the Enraf-Nonius Structure Determination Package) resulted in the quick

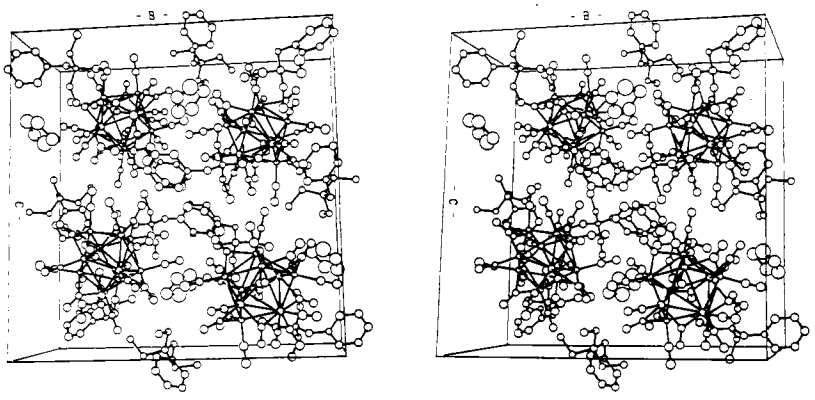

Figure 2. Stereoviews of the unit cell of $[C_6H_5CH_2N(C_2H_5)_3]_3[Rh_{10}As(CO)_{22}]\cdot C_4H_8O$.

Table I. Data for the X-ray Diffraction Study of $[C_6H_5CH_2N(C_2H_5)_3]_3[Rh_{10}As(CO)_{22}]\cdot C_4H_8O$

(a) Crystal Data

cryst system: monoclinic	$\beta = 95.45\ (1)^\circ$
space group: $P2_1/n$	$V = 7642.3$ Å^3
$a = 14.785\ (2)$ Å	$T = 23$ °C
$b = 22.495\ (7)$ Å	$Z = 4$
$c = 23.083\ (5)$ Å	mol wt = 2369.29
$\alpha = \gamma = 90^\circ$	ρ(calcd) = 2.059 g/cm^3

(b) Intensity Data

radiation: Mo Kα
monochromator: graphite crystalline, incident beam
max 2θ: 45°
min 2θ: 0.5°
scan type: θ–2θ
scan range: symmetrical, $[2\theta + \Delta(\alpha_2-\alpha_1)]^\circ$
reflctns collected: 9013 total; 8827 independent
linear abs coeff: 25.65 cm^{-1}; absorption corrections made with the technique (see text)

determination of the position of the 10 rhodium and the arsenic atoms. These atoms were included in full-matrix least-squares refinement resulting in agreement factors of $R_F = 17.8\%$ and $R_{wF} = 26.6\%$. A Fourier synthesis then led to the unambiguous location of all remaining nonhydrogen atoms.

The analysis was continued by using 3093 reflections having $|F_o|^2 > 3\sigma_{|F_o|^2}$. Refinement of positional and anisotropic thermal parameters for all nonhydrogen atoms led to convergence with $R_F = 5.4\%$ and $R_{wF} = 6.0\%$, for a total of 102 nonhydrogen atoms with a number of variable parameters of 464, resulting in a value of 1.272 for the esd of an observation of unit weight with a maximum parameter shift of 1.1 esd on the solvent molecule and of 0.1 esd on the rest of the structure. The function $\sum w(|F_o| - |F_c|)^2$ showed no appreciable dependence either upon $\lambda^{-1}\sin\theta$ or upon $|F_o|$, and the weighting scheme is thus acceptable. In addition, the final difference-Fourier map showed no residual electron density as high as carbon atoms on a previous difference-Fourier map, as indicated by a value of 0.92 e/Å^3 for the absolute height of the residual peaks. A table of observed and calculated structure factor amplitudes is available. Positional parameters are collected in Table II.

Results and Discussion

The formation of $[Rh_{10}As(CO)_{22}]^{3-}$ is an obvious consequence of the loss of the three phenyl radicals initially present in triphenylarsine, in the same way in which the formation of $[Rh_9P(CO)_{21}]^{2-}$ and $[Rh_{10}P(CO)_{22}]^{3-}$ was indicative of the same overall behavior for triphenylphosphine.[3,19] It appears from these results that the similarity in the reactivity of phosphorus- and arsenic-containing ligands already noted under mild conditions[9] is also present in our cases. The cleavage of the arsenic–carbon (sp^2) bond under the same conditions previously used to cleave the same linkage in the case of phosphorus is consistent with the weaker characteristic of the former bond. The ready formation of $As_3Co(CO)_3$ from $(AsCH_3)_5$ under mild conditions[13] suggests that a similar reaction could occur under our conditions. In this case, the formation of $[Rh_{10}As(CO)_{22}]^{3-}$, or similar species, could also happen with species containing arsenic–carbon (sp^3) linkages.

The formation of complexes by the arsenic ligands (Figure 3) in which the arsenic donor centers share up to three valence-shell electrons (I–IV) is also found with phosphorus and sulfur.[2,3] Similarly, the formation by coordinated *atomic arsenic* of three two-center, two-electron bonds (V–VIII) also finds precedent in compounds of the two latter elements.[2,3] The versatility of atomic arsenic as a ligand also results in complexes in which it shares all its valence-shell electrons (IX–XI). The first one, IX, shows an arsenic atom with an oxidation state of I, in a coordination complex not reported with other main-group elements. Instead, the existence of the phosphorus analogues of X and XI is known. In the latter instance, the heteroatom is able to share all outer-shell electrons by formation of a dative bond to a metal center.

The ability of the main-group atoms to share all their valence-shell electrons has been found with non-closo and closo polyhedra. The known examples of the first type of species are $[Co_3(CO)_8(\mu_4\text{-E})]$ (E = P, As)[15,25] and $[Fe_2(CO)_6(\mu$-

Table II. Positional Parameters and Their Estimated Standard Deviations for $[Rh_{10}As(CO)_{22}]^{3-}$ in $[C_6H_5CH_2N(C_2H_5)_3]_3[Rh_{10}As(CO)_{22}]\cdot C_4H_8O$

atom	x	y	z
Rh(1)	0.2372 (2)	0.3100 (1)	0.73476 (10)
Rh(2)	0.5784 (2)	0.2040 (1)	0.65615 (10)
Rh(3)	0.2738 (2)	0.1931 (1)	0.69478 (9)
Rh(4)	0.3078 (2)	0.3106 (1)	0.62474 (10)
Rh(5)	0.3781 (2)	0.2461 (1)	0.80254 (9)
Rh(6)	0.4200 (2)	0.3592 (1)	0.73725 (10)
Rh(7)	0.3966 (2)	0.1957 (1)	0.60757 (9)
Rh(8)	0.4554 (2)	0.1541 (1)	0.73646 (10)
Rh(9)	0.5009 (2)	0.3163 (1)	0.63225 (10)
Rh(10)	0.5564 (2)	0.2685 (1)	0.76309 (10)
As	0.4126 (2)	0.2558 (1)	0.6977 (1)
O(1)	0.093 (1)	0.3782 (9)	0.7902 (9)
O(2)	0.741 (1)	0.1299 (9)	0.6402 (8)
O(3)	0.179 (1)	0.0829 (10)	0.7343 (9)
O(4)	0.169 (2)	0.2903 (11)	0.5266 (10)
O(5)	0.454 (1)	0.2780 (10)	0.9235 (9)
O(6)	0.477 (1)	0.4827 (10)	0.7057 (9)
O(7)	0.315 (1)	0.4118 (10)	0.8299 (9)
O(8)	0.368 (2)	0.2062 (11)	0.4792 (10)
O(9)	0.618 (2)	0.4209 (11)	0.6178 (10)
O(10)	0.666 (1)	0.2422 (10)	0.8743 (9)
O(11)	0.396 (2)	0.0294 (12)	0.7109 (11)
O(12)	0.645 (1)	0.1229 (9)	0.7788 (8)
O(13)	0.576 (2)	0.3809 (10)	0.8248 (10)
O(14)	0.190 (1)	0.4117 (10)	0.6496 (9)
O(15)	0.194 (1)	0.2381 (8)	0.8443 (7)
O(16)	0.085 (1)	0.2391 (10)	0.6709 (9)
O(17)	0.610 (1)	0.2618 (8)	0.5435 (8)
O(18)	0.515 (1)	0.0923 (9)	0.5863 (9)
O(19)	0.734 (1)	0.2813 (9)	0.7151 (8)
O(20)	0.231 (1)	0.1222 (9)	0.5872 (9)
O(21)	0.396 (1)	0.3677 (10)	0.5294 (9)
O(22)	0.378 (1)	0.1232 (10)	0.8478 (9)
C(1)	0.144 (2)	0.350 (1)	0.767 (1)
C(2)	0.680 (2)	0.162 (1)	0.646 (1)
C(3)	0.214 (2)	0.127 (1)	0.721 (1)
C(4)	0.224 (2)	0.299 (1)	0.564 (1)
C(5)	0.422 (2)	0.265 (1)	0.876 (1)
C(6)	0.448 (2)	0.437 (1)	0.716 (1)
C(7)	0.336 (2)	0.382 (1)	0.790 (1)
C(8)	0.379 (2)	0.201 (2)	0.530 (1)
C(9)	0.572 (2)	0.381 (2)	0.621 (1)
C(10)	0.624 (2)	0.250 (1)	0.830 (1)
C(11)	0.422 (2)	0.075 (1)	0.723 (1)
C(12)	0.579 (2)	0.145 (2)	0.757 (1)
C(13)	0.532 (2)	0.352 (2)	0.791 (1)
C(14)	0.233 (2)	0.369 (1)	0.663 (1)
C(15)	0.253 (2)	0.253 (1)	0.812 (1)
C(16)	0.164 (2)	0.245 (1)	0.692 (1)
C(17)	0.577 (2)	0.262 (1)	0.590 (1)
C(18)	0.500 (2)	0.139 (1)	0.608 (1)
C(19)	0.659 (2)	0.264 (1)	0.713 (1)
C(20)	0.279 (2)	0.154 (1)	0.618 (1)
C(21)	0.404 (2)	0.339 (1)	0.578 (1)
C(22)	0.399 (2)	0.158 (1)	0.812 (1)

(20) S. M. Grant and A. R. Manning, *Inorg. Chim. Acta*, **31**, 41 (1978).
(21) G. Huttner and H. G. Schmid, *Angew. Chem., Int. Ed. Engl.*, **14**, 433 (1975).
(22) W. Malisch and R. Janta, *Angew. Chem., Int. Ed. Engl.*, **17**, 211 (1978).
(23) E. Rottinger, and H. Vahrenkamp, *Angew. Chem., Int. Ed. Engl.*, **17**, 273 (1978).
(24) T. Zimler, A. Vizi-Orosz, and L. Marko, *Transition Met. Chem.*, **2**, 97 (1977).
(25) R. S. Gall, A. S. Foust, P. J. Pollock, A. Wojcicki, and L. F. Dahl, Abstracts of the American Crystallographic Association Meeting, Berkeley, Calif., March 1974.

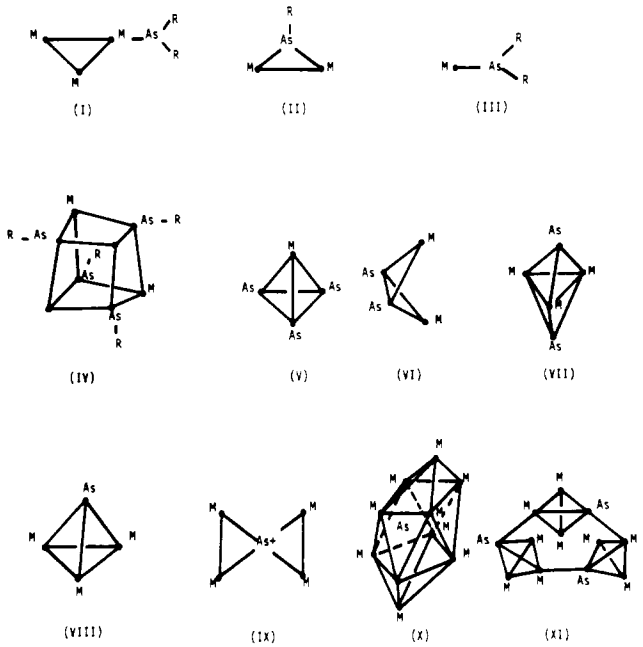

Figure 3. Schematic representation of the different coordination modes of arsenic ligands. Examples are as follows: (I) $Fe_3(CO)_{11}(AsPh(CH_3)_2)$ and $Fe_3(CO)_{11}(As(CH_3)_2CH_2Ph)$;[20] (II) $PhAs[Cr(CO)_5]_2$;[21] (III) $cp(CO)_3MoAs(CH_3)_2$;[22] (IV) $[(CO)_3FeAs(CH_3)]_4$;[23] (V) $As_3Co(CO)_3$;[13] (VI) $Co_2(CO)_6As_2$;[12] (VII) $As_2Fe_3(CO)_9$;[24] (VIII) $[Co_3(CO)_9(\mu_3\text{-As})]$;[18] (IX) $[Co_4(\eta^5\text{-}C_5H_5)_4(CO)_4(\mu_4\text{-As})]^+$;[15] (X) $[Rh_{10}As(CO)_{22}]^{3-}$; (XI) $[Co_3(CO)_8(\mu_4\text{-As})]_3$.[25]

$SCH_3)]_2S$.[26] By contrast, the examples in which the heteroatoms are located inside the cavity of the polyhedra are now pervasive with species reported for carbon (e.g., $[Rh_6(CO)_{15}C]^{2-}$, $[Rh_{15}(C)_2(CO)_{25}]^-$, and others[11a]), sulfur ($[Rh_{17}(S)_2(CO)_{32}]^{3-2}$), nitrogen ($[M_6(CO)_{15}N]^-$ (M = Co, Rh[11b]), phosphorus ($[Rh_9P(CO)_{21}]^{2-3}$ and $[Rh_{10}P(CO)_{22}]^{3-}$[19]), and arsenic ($[Rh_{10}As(CO)_{22}]^{3-}$). The seemingly favorable trend to form clusters with encapsulated main-group heteroatoms may be due to the ability of these atoms to share all their valence-shell electrons with the consequential reduction in the number of ligands located on the cluster's surface, as well as to the effects that the presence of these atoms could induce in the cluster's bonding system.[27]

Structure of the Anion. The structure consists of eight rhodium atoms located on the corners of a cubic antiprism, with the two remaining rhodium atoms found capping the two square faces of the prism (Figure 4). These two atoms and the arsenic atom placed in the geometric center of the cluster form a linear Rh(1)–As–Rh(2) group that defines an angle of 177.3°. This group is located on the idealized C_4 axis of symmetry passing through these atoms.

The average rhodium–rhodium close contacts of the cluster are in the range regularly reported for these compounds.[11] The shortest distances of 2.869 and 2.895 Å are found around the apical rhodium atoms and around the interplanar section. The longer interactions of this type, 3.120 Å, are those along the edges of the basal squares, which show an average value of 90.00 (8)° for the angle between two adjacent edges. The arsenic atom is located on the geometric center of the cluster as indicated by the angles involving this atom and the fact that it is equidistant from the surrounding rhodium atoms. The arsenic–rhodium distances involving the apical rhodium atoms, 3.008 Å, are appreciably longer than those corresponding to the remaining metal atoms, 2.502 Å. This latter interaction is appreciably shorter than the sum of the covalent radii of the two elements, 2.60 Å.[10] In fact, a similar behavior has been observed with other arsenic–transition-metal complexes.

The carbonyl ligands are distributed in a group of 10 terminal carbonyls, one bonded to each rhodium atom, another group of eight bridge carbonyls distributed in two sets of four ligands around each of the apical rhodium atoms, and, finally, another set of four bridging carbonyls bonded between the rhodium atoms defining the two square faces (Figure 5). Rhodium–carbon and carbon–oxygen distances (Table III) are within normal literature ranges,[11] in the case of the terminally bonded ligands, with values of 1.83 and 1.16 Å, respectively. A more interesting situation is present for the bridging carbonyls. The set of these ligands located on the central section of the cluster consists of symmetrically bonded CO (Δ(Rh–C) = 0.04 Å) with normal average rhodium–carbon and carbon–oxygen distances of 1.99 and 1.21 Å, respectively. By

Table III. Interatomic Distances and Esd's for $[Rh_{10}As(CO)_{22}]^{3-}$ (Å)

(a) Rhodium–Rhodium and Rhodium–Arsenic Distances			
Rh(1)–Rh(3)	2.857 (3)	Rh(3)–Rh(8)	2.900 (3)
Rh(1)–Rh(4)	2.836 (3)	Rh(4)–Rh(7)	2.942 (3)
Rh(1)–Rh(5)	2.871 (3)	Rh(4)–Rh(9)	2.847 (3)
Rh(1)–Rh(6)	2.916 (3)	Rh(5)–Rh(8)	2.872 (3)
Rh(2)–Rh(7)	2.818 (3)	Rh(5)–Rh(10)	2.913 (3)
Rh(2)–Rh(8)	2.940 (3)	Rh(6)–Rh(9)	2.964 (3)
Rh(2)–Rh(9)	2.806 (4)	Rh(6)–Rh(10)	2.890 (3)
Rh(2)–Rh(10)	2.908 (3)	Rh(1)–As	3.060 (4)
Rh(3)–Rh(4)	3.163 (3)	Rh(3)–As	2.486 (4)
Rh(3)–Rh(5)	3.042 (3)	Rh(4)–As	2.501 (4)
Rh(4)–Rh(6)	3.142 (3)	Rh(5)–As	2.529 (4)
Rh(5)–Rh(6)	3.051 (3)	Rh(6)–As	2.496 (4)
Rh(7)–Rh(8)	3.161 (3)	Rh(2)–As	2.956 (4)
Rh(7)–Rh(9)	3.146 (3)	Rh(7)–As	2.474 (3)
Rh(8)–Rh(10)	3.010 (3)	Rh(8)–As	2.517 (4)
Rh(9)–Rh(10)	3.237 (3)	Rh(9)–As	2.493 (4)
Rh(3)–Rh(7)	2.836 (3)	Rh(10)–As	2.503 (3)
(b) Rhodium–Carbon Distances			
Terminal Carbonyls			
Rh(1)–C(1)	1.86 (3)	Rh(6)–C(6)	1.87 (3)
Rh(2)–C(2)	1.81 (3)	Rh(7)–C(8)	1.80 (4)
Rh(3)–C(3)	1.87 (3)	Rh(8)–C(11)	1.85 (3)
Rh(4)–C(4)	1.79 (3)	Rh(9)–C(9)	1.82 (4)
Rh(5)–C(5)	1.80 (3)	Rh(10)–C(10)	1.80 (3)
Bridging Carbonyls			
Rh(1)–C(7)	2.45 (3)	Rh(5)–C(15)	1.89 (3)
Rh(1)–C(14)	1.98 (3)	Rh(5)–C(22)	2.01 (3)
Rh(1)–C(15)	2.19 (3)	Rh(6)–C(7)	1.89 (3)
Rh(1)–C(16)	2.02 (3)	Rh(6)–C(13)	1.97 (3)
Rh(2)–C(12)	2.68 (3)	Rh(7)–C(18)	2.00 (3)
Rh(2)–C(17)	2.01 (3)	Rh(7)–C(20)	2.00 (3)
Rh(2)–C(18)	2.12 (3)	Rh(8)–C(12)	1.85 (3)
Rh(2)–C(19)	2.16 (3)	Rh(8)–C(22)	2.00 (3)
Rh(3)–C(16)	1.99 (2)	Rh(9)–C(17)	1.99 (3)
Rh(3)–C(20)	2.00 (3)	Rh(9)–C(21)	1.89 (3)
Rh(4)–C(14)	1.98 (3)	Rh(10)–C(13)	2.04 (4)
Rh(4)–C(21)	1.97 (3)	Rh(10)–C(19)	1.99 (3)
(c) Carbon–Oxygen Distances			
Terminal Carbonyls			
C(1)–O(1)	1.16 (3)	C(6)–O(6)	1.15 (3)
C(2)–O(2)	1.17 (3)	C(11)–O(11)	1.13 (3)
C(3)–O(3)	1.17 (3)	C(8)–O(8)	1.17 (3)
C(4)–O(4)	1.16 (3)	C(9)–O(9)	1.14 (4)
C(5)–O(5)	1.19 (3)	C(10)–O(10)	1.17 (3)
Bridging Carbonyls			
C(7)–O(7)	1.20 (3)	C(17)–O(17)	1.22 (3)
C(12)–O(12)	1.17 (3)	C(18)–O(18)	1.18 (3)
C(13)–O(13)	1.16 (3)	C(19)–O(19)	1.17 (3)
C(14)–O(14)	1.18 (3)	C(20)–O(20)	1.19 (3)
C(15)–O(15)	1.25 (3)	C(21)–O(21)	1.28 (3)
C(16)–O(16)	1.23 (3)	C(22)–O(22)	1.21 (3)

(26) J. M. Coleman, A. Wojcicki, P. J. Pollick, and L. F. Dahl, *Inorg. Chem.*, **6**, 1236 (1967).
(27) J. W. Lauher, *J. Am. Chem. Soc.*, **101**, 2604 (1979).

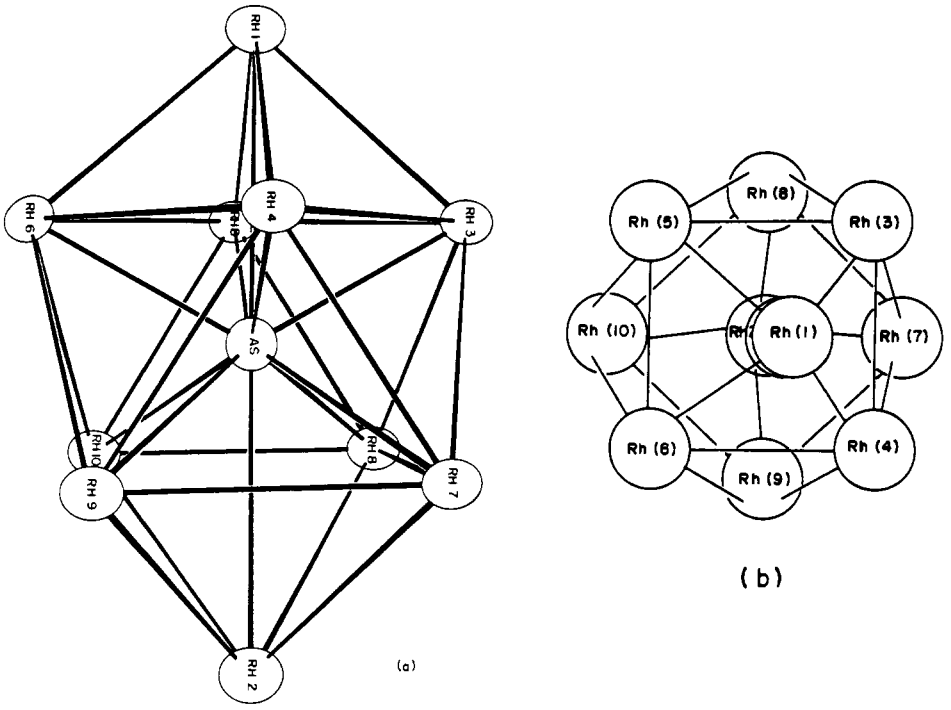

Figure 4. (a) ORTEP diagram of $[Rh_{10}As(CO)_{22}]^{3-}$ with the carbonyl ligands omitted. (b) Schematic view of the rhodium core along an axis that forms an angle of 11° with the fourfold symmetry axis passing through Rh(1)–As–Rh(2).

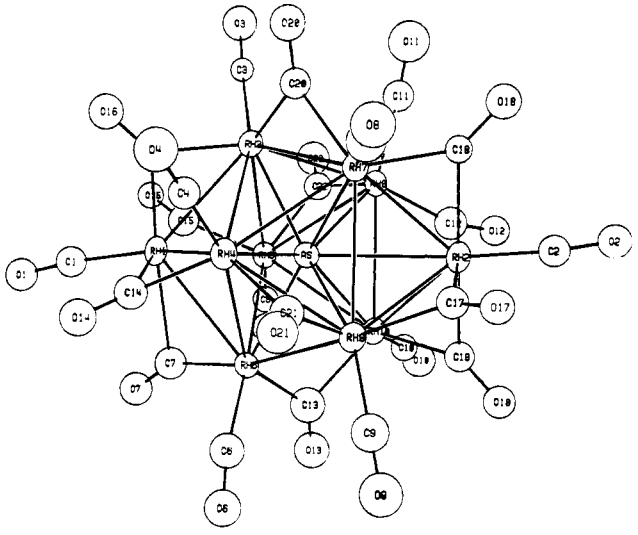

Figure 5. ORTEP diagram of $[Rh_{10}As(CO)_{21}]^{3-}$ with the carbonyl ligands included.

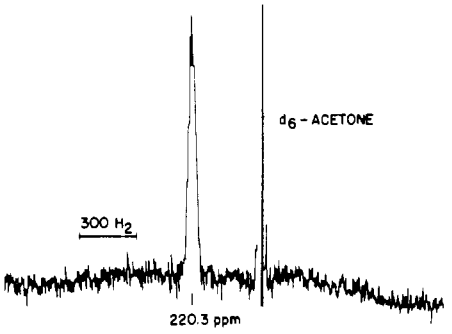

Figure 6. ^{13}C NMR of $[Rh_{10}As(CO)_{22}]^{3-}$ obtained at 40 °C with a sample of the $[PhCH_2N(C_2H_5)_3]^+$ salt in perdeuterioacetone solution after enrichment for 72 h at 25 °C under 1 atm of 50% carbon-13 monoxide.

Chart I

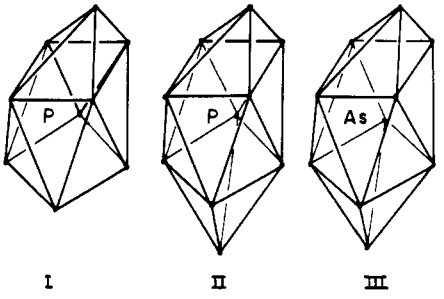

contrast, the ligands surrounding the apical rhodium atoms are asymmetric bridging carbonyls (Δ(Rh–C) = 0.257 and 0.285 Å, for those coordinated to Rh(1) and Rh(2), respectively) with average rhodium–carbon distances of 2.195 and 1.938 Å for the Rh(1)–C and Rh(3)–, Rh(4)–, Rh(5)–, Rh(6)–C interactions and of 2.243 and 1.958 Å for the corresponding lengths around Rh(2). These bond lengths and those of the corresponding carbon–oxygen bonds, 1.215 and 1.185 Å, respectively, are within usual ranges observed for this type of ligand in clusters.

The carbonyl ligands are fluxional between 0 and 60°, as indicated by the presence of a broad multiplet at 220.3 ppm downfield from tetramethylsilane (Figure 6). Similar fluxionality has been found for $[Rh_9P(CO)_{21}]^{2-}$ and $[Rh_{10}P(CO)_{22}]^{3-}$. A study of the fluxionality of the ligands in these and related clusters in a wider thermal range is under way.

Structural Comparison with Other Similar Clusters. The similarities between the structures of $[Rh_9P(CO)_{21}]^{2-}$, $[Rh_{10}P(CO)_{22}]^{3-}$, and $[Rh_{10}As(CO)_{22}]^{3-}$ are apparent from the presence of a common structural polyhedral unit, the square antiprism (see Chart I).

A comparison of the structural parameters of I and II shows that the increase of the degree of reduction of the cluster by one negative charge does not significantly alter the structures of the clusters when it occurs together with the formal addition of a "Rh–CO" group. By contrast, the replacement of phosphorus by arsenic in the otherwise identical clusters II and III results in an elongation of the interplanal rhodium–rhodium contacts corresponding to the edges of the basal squares from

Table IV. Main Angles with Esd's within the Metal Skeleton of $[Rh_{10}As(CO)_{22}]^{3-}$ (Deg)

(a) Rhodium–Rhodium–Rhodium Angles

Rh(3)-Rh(1)-Rh(4)	67.50 (8)	Rh(5)-Rh(3)-Rh(8)	57.73 (7)	Rh(8)-Rh(5)-Rh(10)	62.70 (8)	Rh(2)-Rh(9)-Rh(7)	56.18 (8)
Rh(3)-Rh(1)-Rh(5)	64.16 (8)	Rh(5)-Rh(3)-Rh(4)	89.87 (9)	Rh(1)-Rh(6)-Rh(4)	55.68 (7)	Rh(2)-Rh(9)-Rh(10)	56.99 (8)
Rh(4)-Rh(1)-Rh(6)	66.21 (8)	Rh(7)-Rh(3)-Rh(8)	66.86 (8)	Rh(1)-Rh(6)-Rh(5)	57.47 (8)	Rh(3)-Rh(8)-Rh(5)	63.62 (8)
Rh(5)-Rh(1)-Rh(6)	63.63 (8)	Rh(1)-Rh(4)-Rh(3)	56.57 (8)	Rh(4)-Rh(6)-Rh(5)	90.11 (9)	Rh(3)-Rh(8)-Rh(7)	55.60 (7)
Rh(3)-Rh(1)-Rh(6)	98.72 (9)	Rh(1)-Rh(4)-Rh(6)	58.12 (7)	Rh(4)-Rh(6)-Rh(9)	55.48 (7)	Rh(5)-Rh(8)-Rh(10)	59.32 (8)
Rh(4)-Rh(1)-Rh(5)	100.37 (9)	Rh(3)-Rh(4)-Rh(6)	88.02 (8)	Rh(5)-Rh(6)-Rh(10)	58.64 (7)	Rh(7)-Rh(8)-Rh(10)	91.46 (8)
Rh(7)-Rh(2)-Rh(8)	66.55 (8)	Rh(3)-Rh(4)-Rh(7)	55.22 (7)	Rh(9)-Rh(6)-Rh(10)	67.12 (8)	Rh(4)-Rh(9)-Rh(6)	65.43 (8)
Rh(7)-Rh(2)-Rh(9)	68.01 (9)	Rh(6)-Rh(4)-Rh(9)	59.07 (7)	Rh(2)-Rh(7)-Rh(9)	55.82 (8)	Rh(4)-Rh(9)-Rh(7)	58.56 (8)
Rh(8)-Rh(2)-Rh(10)	61.94 (8)	Rh(7)-Rh(4)-Rh(9)	65.81 (9)	Rh(2)-Rh(7)-Rh(8)	58.58 (7)	Rh(6)-Rh(9)-Rh(10)	55.35 (7)
Rh(9)-Rh(2)-Rh(10)	68.99 (9)	Rh(1)-Rh(5)-Rh(6)	58.90 (8)	Rh(3)-Rh(7)-Rh(4)	66.35 (8)	Rh(5)-Rh(10)-Rh(8)	57.98 (7)
Rh(7)-Rh(2)-Rh(10)	101.03 (9)	Rh(1)-Rh(5)-Rh(3)	57.70 (8)	Rh(3)-Rh(7)-Rh(8)	57.54 (7)	Rh(6)-Rh(10)-Rh(5)	63.44 (8)
Rh(8)-Rh(2)-Rh(9)	101.69 (9)	Rh(6)-Rh(5)-Rh(3)	91.94 (8)	Rh(4)-Rh(7)-Rh(9)	55.64 (7)	Rh(6)-Rh(10)-Rh(9)	57.53 (7)
Rh(1)-Rh(3)-Rh(4)	55.93 (7)	Rh(6)-Rh(5)-Rh(10)	57.92 (7)	Rh(9)-Rh(7)-Rh(8)	89.94 (8)	Rh(2)-Rh(10)-Rh(8)	59.56 (8)
Rh(1)-Rh(3)-Rh(5)	58.14 (3)	Rh(3)-Rh(5)-Rh(8)	58.65 (7)	Rh(2)-Rh(8)-Rh(7)	54.87 (7)	Rh(2)-Rh(10)-Rh(9)	54.02 (8)
Rh(4)-Rh(3)-Rh(7)	58.43 (7)			Rh(2)-Rh(8)-Rh(10)	58.50 (8)		

(b) Angles Involving the As Atom

Rh(1)-As-Rh(2)	177.3 (1)	Rh(2)-As-Rh(6)	118.5 (1)	Rh(5)-Rh(1)-As	50.35 (7)	Rh(4)-Rh(6)-As	51.12 (9)
Rh(1)-As-Rh(3)	60.98 (9)	Rh(3)-As-Rh(4)	78.7 (1)	Rh(6)-Rh(1)-As	49.31 (8)	Rh(5)-Rh(6)-As	53.10 (9)
Rh(1)-As-Rh(4)	60.33 (9)	Rh(3)-As-Rh(5)	74.7 (1)	Rh(7)-Rh(2)-As	50.68 (8)	Rh(2)-Rh(7)-As	67.5 (1)
Rh(1)-As-Rh(5)	60.95 (9)	Rh(4)-As-Rh(6)	77.9 (1)	Rh(8)-Rh(2)-As	50.53 (8)	Rh(8)-Rh(7)-As	51.30 (9)
Rh(1)-As-Rh(6)	62.34 (9)	Rh(5)-As-Rh(6)	74.8 (1)	Rh(9)-Rh(2)-As	51.20 (8)	Rh(9)-Rh(7)-As	50.98 (9)
Rh(1)-As-Rh(7)	115.9 (1)	Rh(7)-As-Rh(8)	78.6 (1)	Rh(10)-Rh(2)-As	50.54 (8)	Rh(2)-Rh(8)-As	65.05 (1)
Rh(1)-As-Rh(8)	117.0 (1)	Rh(7)-As-Rh(9)	78.6 (1)	Rh(1)-Rh(3)-As	69.5 (1)	Rh(7)-Rh(8)-As	50.11 (8)
Rh(1)-As-Rh(9)	117.3 (1)	Rh(8)-As-Rh(10)	73.7 (1)	Rh(4)-Rh(3)-As	50.86 (9)	Rh(10)-Rh(8)-As	52.97 (9)
Rh(1)-As-Rh(10)	118.7 (1)	Rh(9)-As-Rh(10)	80.8 (1)	Rh(5)-Rh(3)-As	53.30 (9)	Rh(2)-Rh(9)-As	67.5 (1)
Rh(2)-As-Rh(7)	61.78 (9)	Rh(3)-As-Rh(6)	123.1 (1)	Rh(1)-Rh(4)-As	69.64 (9)	Rh(7)-Rh(9)-As	50.44 (9)
Rh(2)-As-Rh(8)	64.42 (9)	Rh(4)-As-Rh(5)	121.3 (1)	Rh(3)-Rh(4)-As	50.41 (9)	Rh(10)-Rh(9)-As	49.76 (9)
Rh(2)-As-Rh(9)	61.30 (9)	Rh(7)-As-Rh(10)	125.2 (1)	Rh(6)-Rh(4)-As	50.97 (9)	Rh(2)-Rh(10)-As	65.72 (9)
Rh(2)-As-Rh(10)	63.74 (9)	Rh(8)-As-Rh(9)	125.7 (1)	Rh(1)-Rh(5)-As	68.7 (1)	Rh(8)-Rh(10)-As	53.37 (9)
Rh(2)-As-Rh(3)	118.4 (1)	Rh(3)-Rh(1)-As	49.53 (8)	Rh(3)-Rh(5)-As	52.00 (9)	Rh(9)-Rh(10)-As	49.48 (8)
Rh(2)-As-Rh(4)	117.1 (1)	Rh(4)-Rh(1)-As	50.03 (8)	Rh(6)-Rh(5)-As	52.13 (9)		
Rh(2)-As-Rh(5)	121.7 (1)			Rh(1)-Rh(6)-As	68.3 (1)		

(c) Angles Involving Carbon Monoxide

Terminal Carbonyl

Rh(1)-C(1)-O(1)	173 (3)	Rh(4)-C(4)-O(4)	178 (2)	Rh(7)-C(8)-O(8)	179 (3)	Rh(9)-C(9)-O(9)	176 (3)
Rh(2)-C(2)-O(2)	174 (3)	Rh(5)-C(5)-O(5)	178 (2)	Rh(8)-C(11)-O(11)	173 (3)	Rh(10)-C(10)-O(10)	175 (3)
Rh(3)-C(3)-O(3)	175 (2)	Rh(6)-C(6)-O(6)	171 (3)				

Rhodium–Bridge Carbonyls

Rh(1)-C(16)-O(16)	136 (2)	Rh(2)-C(18)-O(18)	136 (2)	Rh(6)-C(13)-O(13)	140 (3)	Rh(3)-C(16)-O(16)	134 (2)
Rh(1)-C(7)-O(7)	126 (2)	Rh(2)-C(19)-O(19)	134 (2)	Rh(10)-C(13)-O(13)	128 (3)	Rh(5)-C(15)-O(15)	143 (2)
Rh(1)-C(14)-O(14)	134 (2)	Rh(3)-C(20)-O(20)	136 (2)	Rh(5)-C(22)-O(22)	132 (2)	Rh(7)-C(18)-O(18)	138 (2)
Rh(1)-C(15)-O(15)	128 (2)	Rh(7)-C(20)-O(20)	134 (2)	Rh(8)-C(22)-O(22)	136 (2)	Rh(8)-C(12)-O(12)	157 (3)
Rh(2)-C(12)-O(12)	138 (2)	Rh(4)-C(21)-O(21)	129 (2)	Rh(6)-C(7)-O(7)	151 (3)	Rh(9)-C(17)-O(17)	137 (2)
Rh(2)-C(17)-O(17)	134 (2)	Rh(9)-C(21)-O(21)	136 (2)	Rh(4)-C(14)-O(14)	137 (3)	Rh(10)-C(19)-O(19)	137 (2)

(d) Rhodium–Carbon–Rhodium Angles

Rh(1)-C(7)-Rh(6)	83 (1)	Rh(1)-C(16)-Rh(3)	91 (1)	Rh(2)-C(18)-Rh(7)	86 (1)	Rh(4)-C(21)-Rh(9)	95 (1)
Rh(1)-C(14)-Rh(4)	88 (1)	Rh(2)-C(12)-Rh(8)	88 (1)	Rh(2)-C(19)-Rh(10)	89 (1)	Rh(5)-C(22)-Rh(8)	92 (1)
Rh(1)-C(15)-Rh(5)	89 (1)	Rh(2)-C(17)-Rh(9)	89 (1)	Rh(3)-C(20)-Rh(7)	90 (1)	Rh(6)-C(13)-Rh(10)	92 (2)

3.01 to 3.12 Å. This change occurs with an associated increase in the average Rh(plane)–Rh(apical)–Rh(plane) angles opposite to the square diagonals from 98.4° in II to 100.4° in III. If these differences are considered to be significant, they indicate that the increase in the steric demands of the central atom is probably accommodated by the clusters by expansion of the polyhedron perpendicularly to the quarternary axis of symmetry.

The structural comparison of these clusters also shows that the ligand crowding initially present in I[3] gets alleviated upon increasing cluster size as in II and III. The addition of a new rhodium atom results in a drastic change in the carbonyl distribution. Formally, it looks as if the carbonyl ligands located on the most crowded region of I, the basal plane,[3] could tend to relieve their constraints by rearranging around the new apical rhodium atom present in II and III. Another effect possibly also associated with the increase in the size of these clusters is the transformation of the asymmetric bridge ligands of I into symmetrical bridges in II and III. The constancy of the lengths for the rhodium–rhodium edges bridged by carbonyl ligands in I, II, and III indicates that the changes in the symmetry of the bridge carbonyls are not a consequence of an increase in rhodium–rhodium contacts. It appears that these changes may be caused instead by the decrease in the steric demands of the carbonyl ligands.

The structure of $[Rh_{10}As(CO)_{22}]^{3-}$ shows the ability of the basic cluster polyhedron, the square antiprism, to accommodate in the inside of the cluster atoms of size similar to that of arsenic. This is in contrast with previous predictions of the radii of the cluster cavities in the case of rhodium which suggested that neither the square antiprism nor the cube, with cavity radii of 0.90 and 1.02 Å, respectively,[11] should be expected to accommodate atoms as large as arsenic (covalent radius 1.24 Å)[10] if a closo polyhedron is to be maintained. The persistence of the square antiprism as the basic structural building block for closo rhodium carbonyl clusters containing main-group atom(s) inside their cavity is confirmed now for carbon,[28] phosphorus,[3,19] arsenic, and sulfur,[2] with covalent radii in the range 0.77–1.24 Å.

Behavior under High Pressure of Carbon Monoxide. The behavior of rhodium carbonyl clusters under carbon mon-

(28) L. A. Cosby, R. A. Fiato, and J. L. Vidal, U. S. Patent 4 115 433 (1978).

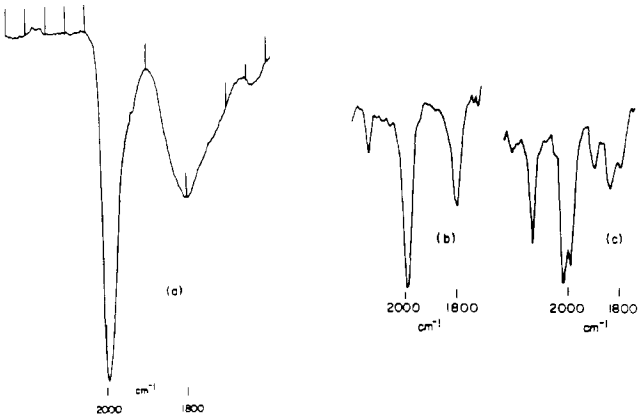

Figure 7. Infrared spectra of $[Rh_{10}As(CO)_{22}]^{3-}$ in solutions of sulfolane (tetrahydrothiophene 1,1-dioxide): (a) at ambient conditions; (b) under 537 atm of $CO-H_2$ at 150 °C; (c) under 862 atm of $CO-H_2$ at 150 °C.

oxide–hydrogen mixtures has attracted our attention for some time[28-30] in an attempt to understand their role in the homogeneous catalytic conversion of $CO-H_2$ into oxygenated organic products.[31-35] These studies have relied mainly on the use of infrared spectroscopy when conducted under high pressure.[4] They show that $[Rh_{10}As(CO)_{22}]^{3-}$ is stable under 537 atm of $CO-H_2$ (1:1 ratio) up to 150 °C as indicated by comparison of the infrared pattern of the anion under ambient and at the former conditions (Figure 7). An increase in the pressure to 862 atm results in spectral changes (Figure 7) that are indicative of the presence of other carbonyl-containing species together with the initial anion. The absorption at 1895 cm^{-1} (± 5 cm^{-1}) probably belongs to $[Rh(CO)_4]^-$,[4] while the remaining new bands at 2010 and 1830 cm^{-1} resemble those previously assigned to $[Rh_9P(CO)_{21}]^{2-}$.[3] The existence of an arsenic-containing analogue of the latter cluster is plausible and the following reaction can be proposed on the basis of a similar reaction for $[Rh_{10}P(CO)_{22}]^{3-}$.[19]

$$[Rh_{10}As(CO)_{22}]^{3-} + 3CO \rightleftharpoons [Rh_9As(CO)_{21}]^{2-} + [Rh(CO)_4]^-$$
$$1990,\ 1815\ cm^{-1} \qquad 2010,\ 1835\ cm^{-1} \qquad 1895\ cm^{-1}$$

We have been able to isolate and characterize $[Rh_9As(CO)_{21}]^{2-}$, confirming the tentative assignment of the infrared pattern above.[36]

Acknowledgment. The publication approval of this work by Union Carbide Corp. is appreciated. The continuous encouragement received from Dr. G. L. O'Connor is also recognized. The NMR spectra were obtained by Dr. R. C. Schoening and the high-pressure infrared spectra by Dr. W. E. Walker, both of Union Carbide Corp. at this location.

Registry No. $[PhCH_2N(C_2H_5)_3]_3[Rh_{10}As(CO)_{22}]\cdot C_4H_8O$, 75802-04-9; $[C_6H_5CH_2N(C_2H_5)_3]_2[Rh_9As(CO)_{21}]$, 75802-02-7; $[Rh(CO)_4]^-$, 44797-04-8; $Rh(CO)_2acac$, 14874-82-9; Ph_3As, 603-32-7.

Supplementary Material Available: Complete listings of structural factors, thermal and positional parameters, and interatomic distances and angles (60 pages). Ordering information is given on any current masthead page.

(29) J. L. Vidal, Z. C. Mester, and W. E. Walker, U. S. Patent 4 115 428 (1978).
(30) J. L. Vidal and W. E. Walker, U. S. Patent 4 180 517 (1979).
(31) J. L. Vidal and J. N. Cawse, U. S. Patent 4 111 975 (1978).
(32) R. L. Pruett and W. E. Walker, U. S. Patent 3 833 634 (1974).
(33) L. Kaplan, U. S. Patent 3 944 588 (1976).
(34) L. Kaplan, German Patents 2559057, 2643913, 2643897, 2743630, and 2823127 (1977).
(35) L. Kaplan and W. E. Walker, German Patent 2643971 (1977).
(36) J. L. Vidal, W. E. Walker, R. C. Schoening, and J. M. Bennett, no reported results.

Contribution from Union Carbide Corporation, South Charleston, West Virginia 25303

Rhodium Carbonyl Cluster Chemistry under High Pressure of Carbon Monoxide and Hydrogen. 3. Synthesis, Characterization, and Reactivity of $HRh(CO)_4$

JOSÉ L. VIDAL* and W. E. WALKER†

Received November 20, 1979

The fragmentation of $Rh_4(CO)_{12}$ in dodecane solutions under 1241–1379 atm of carbon monoxide at 5–12 °C has been established by high-pressure infrared spectroscopy to give $Rh_2(CO)_8$. Noticeable spectral changes are caused by the introduction of small amounts of hydrogen (1542 atm, $CO:H_2 = 4.5:1$). Fourier subtraction of the spectra of these two species left bands at 2070 (m), 2039 (vs), and 2008 (w) cm^{-1}. By analogy to the spectra previously observed for $HIr(CO)_4$ and $HCo(CO)_4$ this pattern is assigned to $HRh(CO)_4$, a species that has eluded previous attempts of detection. The reaction of $[M(CO)_4]^-$ (M = Co, Rh, Ir) with protonic acids in tetraglyme–toluene under high pressure of carbon monoxide resulted in the formation of $HM(CO)_4$ (M = Co, Rh, Ir), with the reaction having been readily detected in the case of iridium with phosphoric acid (Ir:P = 0.38:4.12), while a stronger acid such as sulfuric acid was required for cobalt (Co:S = 0.95:29.9) and rhodium (Rh:S = 0.90:29.4) for the detection of a similar reaction. These results suggest that the proton affinity of these ions varies as $[Ir(CO)_4]^- > [Co(CO)_4]^- > [Rh(CO)_4]^-$. The differences in the acid strength of the corresponding conjugate acids, $HM(CO)_4$ (M = Co, Rh, Ir), was determined under high pressures of $CO-H_2$ by reaction with amines of different basicities such as *N*-methylmorpholine (pK(water, 25 °C) = 7.4) and *N,N*-dimethylaniline (pK(water, 25 °C) = 4.8) after formation of the tetracarbonylmetal hydrides, "in situ." $HIr(CO)_4$ is not deprotonated in a detectable fashion by *N*-methylmorpholine (Ir:N = 1:10), while $HCo(CO)_4$ is deprotonated by this amine (Co:N = 2.4:1.0) but not by *N,N*-dimethylaniline (Co:N = 2.4:3.0). By contrast $HRh(CO)_4$ readily undergoes deprotonation with this amine (Rh:N, = 2.7:1.0). These results correspond to the following trend in Brønsted acidity: $HRh(CO)_4 > HCo(CO)_4 > HIr(CO)_4$.

Introduction

Homogeneous catalysis with transition metals is a rapidly expanding area[1] and several operating industrial processes are now based on these types of catalysts.[2] The elements of the cobalt triad–Co, Rh, and Ir—have probably been the most

† Deceased.

(1) D. Forster and J. E. Roth, Eds., *Adv. Chem. Ser.* No. 70 and 132 (1970 and 1974), and references therein.
(2) G. W. Parshall, *J. Mol. Catal.*, 4, 243 (1979).

0020-1669/81/1320-0249$01.00/0